Journal Name

ARTICLE

Cost-effective side-illumination darkfield nanoplasmonic markers microscopy.

Received 00th January 20xx,
Accepted 00th January 20xx

DOI: 10.1039/x0xx00000x

www.rsc.org/

Mengjiao Qi, Cecile Darviot, Sergiy Patskovsky, * and Michel Meunier

We present the development of an innovative technology for quantitative multiplexed cytology analysis based on the application of spectrally distinctive plasmonic nanoparticles(NPs) as optical probes and on a cost-effective side-illumination multispectral darkfield microscopy (SIM) as differential NPs imaging method. SIM is based on lateral illumination by arrays of discrete color RGB light emitting diodes (LEDs) of spectrally adjusted plasmonic NPs and consecutive detection by the conventional CMOS color camera. We demonstrate the enhanced contrast and higher resolution of our method for individual NPs detection in the liquid medium and of NPs markers attached on cell membrane in a cytology preparation by comparing it to the conventional darkfield microscopy(DFM). The proposed illumination and detection system is compatible with current clinical microscopy equipment used by pathologist and can greatly simplify the adaptation of plasmonic NPs as novel reliable and stable biological multiplexed chromatic markers for biodetection and diagnosis.

Introduction

Over recent years, tremendous efforts have been invested in designing novel nanoparticle(NP) probes with unique properties that are advantageous for the use in biochemical diagnostics and disease treatment[1,2]. The NP probes most widely used in diagnostic applications are quantum dots (QDs), polymer dots (PDs), upconversion nanoparticles (UCNPs), and plasmonic nanoparticles (NPs) [3].

The unique optical and physical properties of plasmonic NPs, their proven photo-stability, water solubility and biocompatibility provide new opportunities and open new fields of biomedical application ranging from using NPs as targeted drug carrier or gene deliverer into cancerous cells, to using NPs as biological immunomarker agent in biomedical diagnostics and disease treatment[4-7]. An outstanding example is the use of spectrally tunable NPs as optical *multiplexing* biomarkers for selective cells and tissues labelling[8, 9]. This multiplexed method could notably show several advantages for cytology applications. Currently, in cytology specimen analysis, pathologists heavily rely on immunohistochemistry (IHC) to increase the accuracy of their diagnosis[10]. Multiple preparation steps have to be performed to color these proteins, which can destroy the proteins and therefore strongly reduces the reliability of the technique. It is also impossible to assess the relative expression of multiple antibodies(Abs) at the single cell level, which is important for a reliable diagnosis. There is a need for a cost-effective, sensitive and specific diagnostic methodology to overcome the limitations associated with conventional IHC based methods. We think that a methodology based on a new cytology protocol, where immunolabeling by plasmonic NPs[11, 12] is done on fresh cells before fixation can improve diagnostic reliability.

To promote user adoption of this new method in cytopathology laboratories, the NPs imaging hardware should be compatible with equipment currently used in laboratories, and the sample preparation and imaging procedure should not involve additional steps or risks of contamination to the sample compared with the existing procedure. This currently represents a challenge with plasmonic NPs markers, as the optical detection of plasmonic NPs typically relies on the scattered light by NPs detected in a darkfield microscopy(DFM) mode. Although there are on the market hyperspectral microscopes with a darkfield condenser to detect and differentiate NPs with a very high resolution (e.g.: CytoViva, Photon Etc.), they are costly, require considerable changes to the conventional microscopy system, and are therefore impractical in clinical settings. Recently, we proposed a widefield hyperspectral 3D imaging of cell-NPs [13] with reflected light microscopy (RLM)[14] which overcomes the numerical aperture (NA) limitations of darkfield imaging and provides enhanced contrast of NPs imaging in cellular environment. However, the RLM requires high NA immersion objectives with

* *Engineering Physics Department, Ecole Polytechnique de Montréal, Laser Processing and Plasmonics Laboratory, Montréal, Québec, H3C 3A7, Canada. E-mail: sergiy.patskovsky@polymtl.ca*

Electronic Supplementary Information (ESI) available. See DOI: 10.1039/x0xx00000x

matching oil that contaminate histopathology and cytology microscopy samples and limit widespread application.

In this article, we propose to use a multispectral side-illumination darkfield microscopy(SIM) method that allows to design and fabricate a compact microscopy module for optical imaging and spectroscopic identification of individual plasmonic NPs in fixed or live cell preparations. This method employs darkfield NPs imaging with lateral optical illumination[15, 16] that removes the inherent limitations on the NA of the imaging objective used for the conventional darkfield microscopy and provides an enhanced contrast of plasmonic NPs in the diffusing medium, cellular membrane and extracellular matrix. By using recent light emitting diode(LED) technology for side-illumination, the dimension of the proposed microscopy module can be comparable with the conventional histopathology sample holder. This compact side-illumination module can provide a convenient and routine method for immunoplasmonic markers visualization by cytopathologists. It can be easily adaptable to the microscopes currently used in the clinical setting thus facilitating and accelerating its adoption.

Experimental

Cell culture

To image NPs mixture in cellular environment, we cultured adherent MDA-MB-231 human breast cancer cells and suspension Y79 human retinoblastoma cells.

MDA-MB-231 cells were grown in Dulbecco's Modified Eagle's Medium (DMEM) containing 10% fetal bovine serum (FBS, Life Technologies) and 1% penicillin and streptomycin (PS, Invitrogen) and cells were removed by trypsinization and seeded onto microscopic slide with help of self-insertion well from Ibidi. When the cells reached ~80% confluence, they were incubated with NPs mixture for ~3 hours in incubator and then washed 3 times with phosphate-buffered saline (PBS, Sigma-Aldrich), fixed with cold methanol for 5 minutes and washed for another 3 times with PBS. Then the self-insert well was replaced by the coverslip (SPI Supplies) on top of the slide.

Y79 cells were cultured in RPMI 1640 (Life Technologies) containing 10% FBS (Life Technologies) supplemented with 1% PS. NPs mixture was incubated with Y79 cells for 3 hours before centrifugation at 200g for 7 minutes. The NPs mixture incubated Y79 cells were then sprayed on a slide coated with poly-L-lysine and covered by a coverslip.

Plasmonic nanoparticles.

For both individual or multiplexed NPs detection applications shown in this article, we used 70nm silver(Ag) spherical NPs (Ted Pella Inc.), 50nm, 60nm and 80nm gold(Au) spherical NPs (Nanopartz), and 40 x 80nm gold nanorods (AuNR) (Nanopartz).

The NPs were placed in different environments to prepare the samples: in homogeneous low-scattering PBS medium and in a high-scattering cellular environment filled with Vectashield Antifade Mounting Medium. We used conventional 25x75 microscopy slides as a substrate with thin 0.13-0.17um coverslips.

Side-illumination microscopy adaptor.

The main principle of the side-illumination darkfield method is shown in Fig.1A and the schematic of the light beam propagation is presented in the Fig.1 of the electronic supplementary information (ESI). Fig.1B shows a technical schematic of the microscopy module with lateral LED illumination. Two types of microscopy adaptors optimized for inverted (Fig.1C) and upright microscopes (Fig.1D) were designed by us and fabricated by VegaPhoton. The adaptors were fabricated with aluminum CNC machining to obtain the precision and rigidity required for use with professional microscopes. To simplify integration, in the case of the inverted microscope, the adaptor was integrated into a ProScan™ flat top inverted microscope motorized stage (Prior Scientific, Inc.) that allows fine 3D spatial sample translation. For the conventional upright microscope, the adaptor thickness was designed to be only 5.4 mm for seamless integration with the existing transmission illumination setup and to avoid hinder to the objective free run. The narrow RGB LED array (2.8 x 0.35 x 0.85, Citizen CL246) is mounted on a PCB card compatible with both inverted and upright microscope and placed in close optical contact with both sides of the standard microscope slides used in histo- and cyto-pathological analysis, as shown in Fig.1B. Typical emission spectra of the RGB LED are shown on the Fig.2A.

The manual or automatic power control of illumination intensity for individual color LED provides possibility for direct visualization of multiple plasmonic biomarkers placed in the medium or on the cellular membrane. Automatic LED intensity control is very useful for the development of the digital NPs imaging and detection using a fast CMOS color or monochromatic camera and sophisticated image treatment software. Another advantage of the proposed microscopy adaptor is in the simplicity of switching between the conventional transmission mode already used by pathologist and the darkfield side-illumination mode and, especially, the possibility to use them together, thus generating more relevant information about investigated samples.

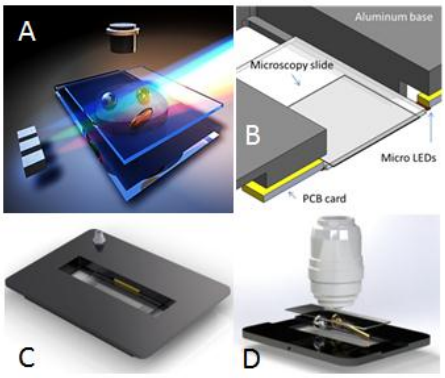

Fig.1 (A) Principle of the side-illumination darkfield technique. (B) Schematics and (C) experimental prototypes of the darkfield microscopy with side LED illumination designed for inverted and (D) upright microscopes.

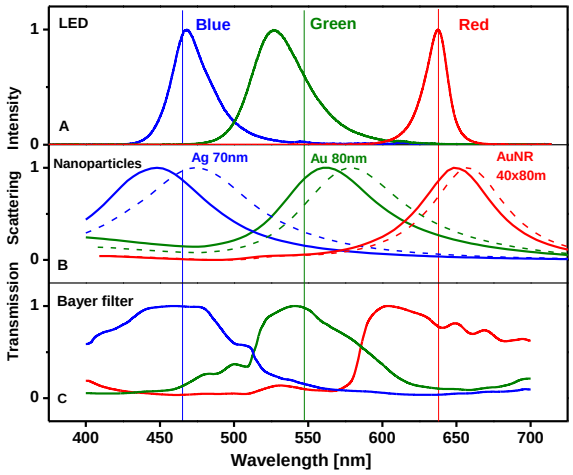

Fig. 2 Resonance peaks of NPs are selected to fit the spectral emission of the color LED used for lateral illumination and to the imaging camera detector filters. (A) CL246 LED spectral emission properties. (B) Scattering properties of 70nm Ag NPs, 80nm Au NPs and 40x80nm Au NRs in PBS (solid line) and in Vectashield mounting medium(dashed line). (C) Transmission spectral profiles of CMOS camera Bayer filters.

Results and discussion

Side-illumination darkfield multispectral plasmonic NPs microscopy.

The proposed SIM method and corresponding microscopy module are based on four complementary technologies, in order to provide a high resolution and high contrast NPs imaging in the complex medium and facilitate integration into existing optical systems.

The first technology is a darkfield microscopy technique based on lateral illumination[15, 17, 18]: this method resides in excluding the non-scattered light from the output image by using an illumination orthogonal to the imaging lens optical axis. This approach is optimal for darkfield NPs imaging contrast and what is also important it removes the inherent limitation on the NA of the objective which has to be smaller than the NA of the illumination condenser in conventional transmission darkfield mode. The second technology is an application of the recent development in discrete color LEDs specifically designed and optimized for lateral illumination of thin glass substrates (<400µm). Such LEDs can be directly put in close optical contact with standard microscope slides and coverslips. The third technology is based on the multiplexing abilities and unique resonance properties of metallic NPs, which demonstrate an enhanced scattering efficiency compared to the cellular membrane. Furthermore, the possibility to tune NPs plasmon peak to the maximum intensity of the illuminating LED source allows to improve the efficiency of NPs chromatic differentiation. The fourth technology relies on the introduction

on the market of a low-cost, fast and sensitive CMOS cameras. Such cameras in combination with corresponding image treatment software serve as the basis for the automatic multiplex NPs detection, spatial localization and spectral differentiation.

As follow from the above description, the most efficient NPs detection system will use matching and as narrow as possible spectral characteristics of LED sources, imaging camera filters and plasmonic NP scattering spectra. However, while it is possible to build such system with the available technology, the cost-efficiency aspect introduces certain limitation on the optical design. In this work we are using a freely available on the market RGB lateral illumination LEDs in combination with a compact low cost color CMOS camera (Ximea). Integrated into the camera Bayer filters provides a relatively large spectral range still giving the opportunity for the multiplexing.

Resonance properties of the plasmonic NPs can be readily tuned to the optimal peak position by changing material, composition, size and geometry. However, a reliable NPs detection by the darkfield method imposes a limitation on the scattering efficiency that directly depends on the NPs size. That is why in this work we are using sufficiently large NPs for the multiplexing: 70nm Ag, 80nm Au, and 40 x 80nm AuNR. On the Fig.2 we show theoretical scattering spectra for our choice of NPs placed in the two most used medium for the visualization: PBS buffer with refractive index(RI) 1.34 and mounting medium with RI=1.45. As we can conclude from the figure, the spectral position of the especially 80nm Au NPs is far from the optimal, but taking in the account of NPs scattering efficiency and CMOS camera sensitivity these NPs can be spectrally differentiated as we show below.

Multispectral plasmonic NPs imaging in homogeneous medium

SIM method using our portable adaptor for inverted microscope (Fig. 1C) was initially used to test the efficiency of the approach in the comparative study with conventional transillumination DFM(Nikon). Plasmonic NPs were placed on the microscopy slide in the PBS bufferdrop and covered by the thin coverslip through the 200um spacer. Objective 60x, 0.7NA was used for the imaging and Nikon darkfield condenser(NA 0.8-0.95) was used for conventional darkfield setup. All RGB LEDs were illuminated for the side-illumination adaptor. On Fig.3 we present results for the detection of Au NPs with different sizes. On the same images we also show a local scattering intensity distribution that allows us to compare experimental signal to- noise ratio and NPs contrast obtained by these two optical methods. As we can conclude from these figures even for the smallest 50nm Au NPs, that we are considering as the limit for the reliable NPs detection, side-illumination mode provides a higher contrast and thus is more performant and has the potential for a reliable NPs detection. The obvious NPs color difference is explained by the different illumination sources: RGB LEDs for side-illumination and halogen for darkfield method.

For the next experiment we prepared a 1x1x1 mixture of three NPs optimal for the SIM mode: 70nm Ag NPs(spectral peak 450nm), 80nm Au NPs (spectral peak 560nm)and 40x80nm Au NRs (spectral peak 650nm). Obtained color images are shown on Fig. 4. All three individual NPs in the homogeneous PBS solution can be discriminated in different scattered colors even by visual observation.

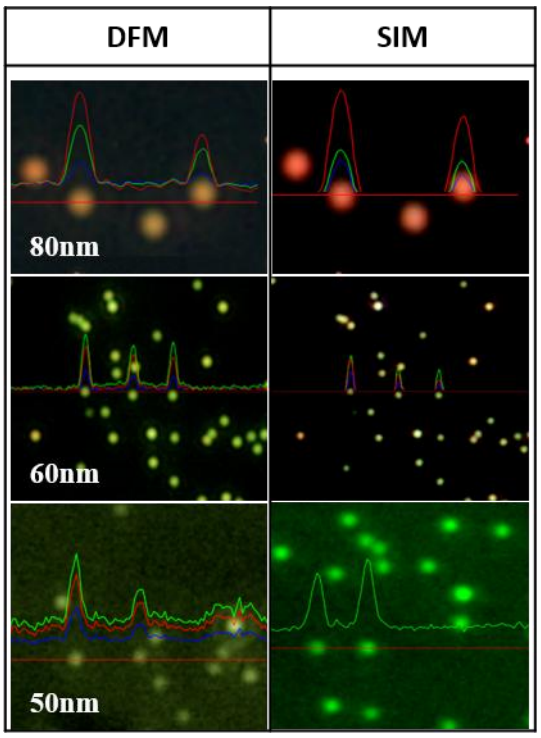

Fig.3. Comparative conventional darkfield microscopy(DFM) with Nikon darkfield condenser (left column) and side-illumination microscopy(SIM)(right column) detection of Au NPs samples with different sizes(80nm, 60nm, 50nm). NPs in the PBS buffer between conventional microscopy slide and thin coverslip. Objective 60x, 0.7NA.

However, a more reliable differentiation method can be proposed by controlling illumination intensities of different LEDs. For example, only Ag NPs was detected with individual LED blue channel on and both of Ag and Au NPs were visualized with blue and green channels on, as presented in Fig. 4B and C. Au NRs can be subtracted from the NPs mixture image taken with all LEDs on, as shown in Fig. 4D.

Plasmonic NPs imaging in cell-NPs complex.

And finally, we are presenting the most important results of multiplexed NPs visualization. Different cell lines with different sizes and properties were nonspecifically decorated with plasmonic NPs and observed by the proposed SIM mode and DFM mode for comparison.

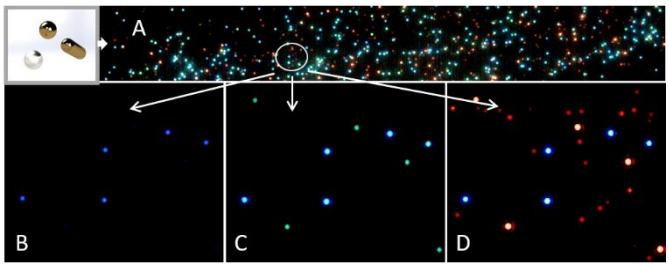

Fig. 4 (A) Example of NPs mixture on a coverslip visualization with SIM microscopy. (B) Magnified Ag NPs imaging with only blue LED, (C) Ag and Au NPs imaging with blue and green LEDs, (D) Ag, Au, Au NR mixture imaging with all LEDs. Objective 60x, 0.7NA.

Firstly, we prepared a cytology sample with MDA-MB-231 that is a highly aggressive, invasive and poorly differentiated triple-negative breast cancer cell line. Triple-negative breast cancer is an aggressive form of breast cancer with limited treatment options. Understanding the molecular basis of this cancer is therefore crucial for effective new drug development and as a result many studies on potentially active agents for this particular type of breast cancer have been conducted using the MDA-MB-231 cell line (PHE Culture Collections)[19, 20]. MDA-MB-231 are rather large (up to 30um) adherent cells. They were mixed with our three types of NPs and placed in the Vectashield antifade mounting medium.

Retinoblastoma is a rare childhood cancer of the eye that can begin in utero and is diagnosed during the first few years of life. To date, two human retinoblastoma cell lines, Weri1 and Y79, are widely used in research. Y79 cell-line is suspension cells with small dimensions (10-12 um diameter) and two markers on the membrane can be selectively labelled by plasmonic probes: MRC2 and CD209[21]. We have prepared a second type of cytology samples with a Y79 cell–NPs complex placed in the mounting medium.

As was shown in the literature[22, 23], the influence of cellular environment on the quality of the conventional dark-field optical detection of the forward scattering light makes image interpretation and NPs visualization in the cellular environment quite complicated or even impossible (Fig.2 in the ESI). However, our experimental results obtained with a SIM setup showed drastic improvement for the NPs visualization in the cellular environment comparing to the conventional darkfield mode. In Fig.5, we present the images of MDA-MB-231 and Y79 cells decorated with different NPs where high NPs contrast allows reliable spatial and spectral detection even by direct visual observation. It is not the case for the DFM where high cellular scattering block NPs. This phenomenon is more obvious for smaller Y79 cells making NPs differentiation and even detection impossible.

NPs spatial distribution and spectral differentiation in cellular environment is a main parameter for using NPs as multiplexed biomarkers to target specific cells in biomedical applications and our results show a good potential for the SIM method to provides a reliable information.

Side-illumination adaptor imposes no limitation on the objective NA, so we can increase a NA up to 0.95. Results of the SIM image of cells-NPs complex taken with objective 60x, 0.95NA with corresponding local 3D NPs intensity patterns confirm high contrast of NPs placed on the cell membrane.

Such advantage of the SIM method is very useful for the application of localizing NPs position in the 3D space. Enhanced spatial resolution especially in the z-direction is provided by the objective with high NA and the experimental result of dynamic 3D NPs scanning is attached in ESI Video.

Our microscopy approach has significantly lower NPs multiplexing capabilities than continuous scanning hyperspectral systems. However, considering a much lower cost, simplicity of integration and utilization in the fields where

three plasmonic markers can provide adequate information,

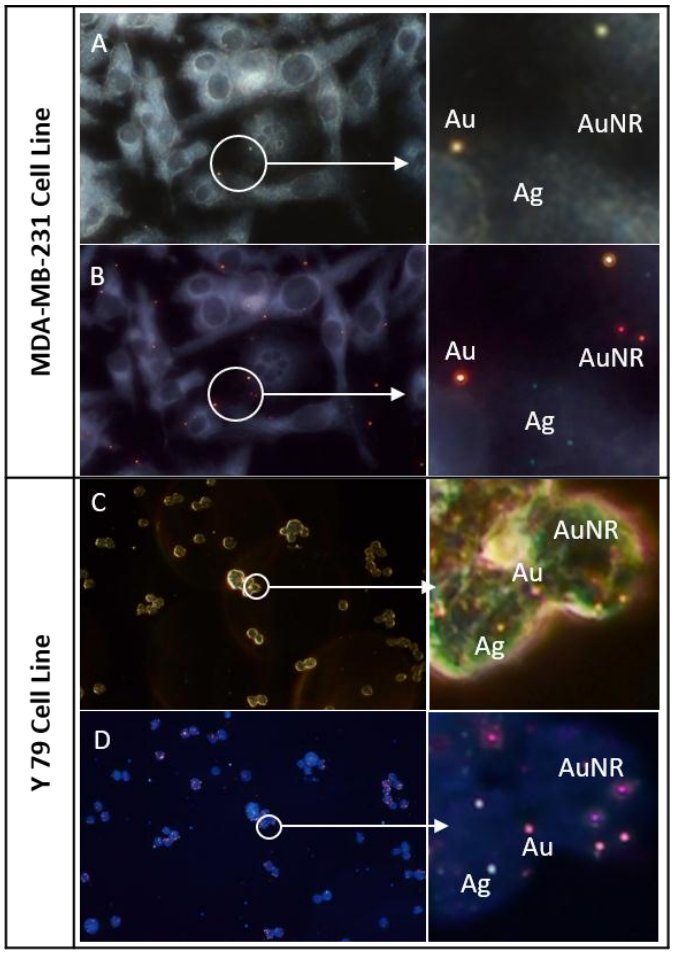

Fig. 5 Cell-NPs complex imaging by DFM (A, C) and SIM (B, D). Adherent cell line MDA-MB-231 (A, B) and suspension cell line Y79 (C, D). Insets show a magnified view of the selected area.

SIM has a very good industrial potential. Also, a continuous advancement of the microelectronic technology will provide new more efficient and spectrally variable LED light sources and imaging detectors with tunable filters that will contribute to the performance of SIM technology.

This compact side-illumination module presented in this work, can provide a convenient and routine method for

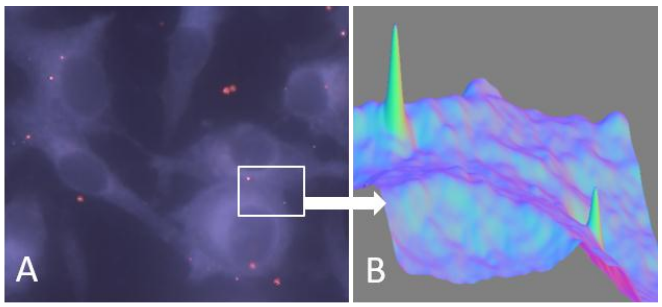

immunoplasmonic markers visualization by the pathologist.

Fig. 6 (A) SIM image of cells-NPs complex taken with objective 60x, 0.95NA. (B) corresponding 3D intensity patterns show high contrast of NPs placed on the MDA-MB-231 cell membrane.

However, to achieve this goal, it is necessary to develop the corresponding hardware architectures and software algorithms, which will automatically detect positions, types and concentration of the immunoplasmonic markers using a multispectral data cube. As the result the SIM method could serve as the basis for the whole slide imaging (WSI) automatic system[24]. Such system will enable pathologists to read slides digitally, helps to visualize/identify new immunoplasmonic biomarker signatures and to develop early diagnosis and effective therapeutic intervention tools. The inherent stability of immunoplasmonic biomarkers (noble metal NPs preserve their plasmonic properties for a long time) can be considered as advantage as the time between labelling and digitization became not critical.

Conclusion

Side-illumination plasmonic nanoparticles microscopy(SIM) has several advantages such as high optical contrast for individual NP imaging, precise 3D NPs localization due to the high NA objectives, possibility of the visual and software-based NPs chromatic differentiation, simple integration on any upright or inverted microscope preserving original functionalities. Pathologists and cytologists would benefit from this cost-effective, portable and functional side illumination setup for their request of real-time diagnosis and test. Combined with the technique of specific antibody functionalized NPs selectively targeting diseased cells, our SIM system can provide a cost-effective, compact clinically relevant approach for quick diagnosis and high efficiency therapeutic treatment.

Conflicts of interest

"There are no conflicts to declare".

Acknowledgement

The authors thank Dr. Pierre Hardy for providing Y79 human retinoblastoma cells for the tests and Yves Drolet for technical support.

References

1. M. A. E.-S. Xiaohua Huang, *Journal of Advanced Research*, 2010, **1**, 15.
2. K. T. Yong, I. Roy, M. T. Swihart and P. N. Prasad, *J Mater Chem*, 2009, **19**, 4655-4672.
3. A. B. Chinen, C. M. Guan, J. R. Ferrer, S. N. Barnaby, T. J. Merkel and C. A. Mirkin, *Chem Rev*, 2015, **115**, 10530-10574.
4. S. Patskovsky, E. Bergeron, D. Rioux, M. Simard and M. Meunier, *The Analyst* 2014, **139**, 5247 - 5253.
5. A. Saha, S. K. Basiruddin, R. Saekar, N. Pradhan and N. R. Jana, *Journal of Physical Chemistry* 2009, **113**.

6. K. Seekell, M. J. Crow, S. Marinakos, J. Ostrander, A. Chilkoti and A. Wax, *Biomedical optics* 2011, **16**.
7. S. Naahidi, M. Jafari, F. Edalat, K. Raymond, A. Khademhosseini and P. Chen, *J Control Release*, 2013, **166**, 182-194.
8. C. C. Wang, C. P. Liang and C. H. Lee, *Appl Phys Lett*, 2009, **95**.
9. X. H. Huang, P. K. Jain, I. H. El-Sayed and M. A. El-Sayed, *Nanomedicine*, 2007, **2**, 681-693.
10. V. Kumar, A. K. Abbas and J. C. Aster, *Robbins & Cotran Pathologic Basis of Disease*, Elsevier Health Sciences, 2015.
11. E. Bergeron, S. Patskovsky, D. Rioux and M. Meunier, *NANOSCALE*, 2016, **8**, 13263-13272.
12. K. Seekell, H. Price, S. Marinakos and A. Wax, *Methods*, 2012, **56**, 310-316.
13. S. Patskovsky, E. Bergeron, D. Rioux and M. Meunier, *Journal of biophotonics* 2015 **8**, 401-407.
14. S. Patskovsky and M. Meunier, *J Biomed Opt*, 2015, **20**.
15. Y. Kawano, C. Higgins, Y. Yamamoto, J. Nyhus, A. Bernard, H. W. Dong, H. J. Karten and T. Schilling, *Plos One*, 2013, **8**.
16. S. Ramachandran, D. A. Cohen, A. P. Quist and R. Lal, *Sci Rep-Uk*, 2013, **3**.
17. J. H. Kim and J. S. Park, *Scientifique Reports* 2015, **5**.
18. M. H. V. Werts, V. Raimbault, M. Loumaigne, L. Griscom, O. Francais, J. R. G. Navarro, A. Debarre and B. Le Pioufle, *Proc Spie*, 2013, **8595**.
19. M. Azizi, H. Ghourchian, F. Yazdian, S. Bagherifam, S. Bekhradnia and B. Nystrom, *Sci Rep-Uk*, 2017, **7**.
20. A. Mukerjee, J. Shankardas, A. P. Ranjan and J. K. Vishwanatha, *Nanotechnology*, 2011, **22**.
21. A. Gallud, D. Warther, M. Maynadier, M. Sefta, F. Poyer, C. D. Thomas, C. Rouxel, O. Mongin, M. Blanchard-Desce, A. Morere, L. Raehm, P. Maillard, J. O. Durand, M. Garcia and M. Gary-Bobo, *Rsc Adv*, 2015, **5**, 75167-75172.
22. R. A. Meyer, *Applied Optics*, 1979, **18**, 585 - 588.
23. Q. Zhang, L. Zhong, P. Tang, Y. Yu, S. Liu, J. Tian and X. Lu, *Scientifique Reports*, 2017, **7**.
24. L. Pantanowitz, P. N. Valenstein, A. J. Evans, K. J. Kaplan, J. D. Pfeifer, D. C. Wilbur, L. C. Collins and T. J. Colgan, *J Pathol Inform*, 2011, **2**, 36.